High-speed, Underwater 3D Imaging with an In-Pixel Histogramming SPAD

Istvan Gyongy[1], Rui Zhang[2], Germán Mora-Martín[1], Robert K. Henderson[1], Gerald Buller[2], Aurora Maccarone[2]
[1]The University of Edinburgh, Institute for Integrated Micro and Nano Systems, Edinburgh, U.K.
[2]Heriot-Watt University, Institute of Photonics and Quantum Sciences, Edinburgh, U.K.
Istvan.Gyongy@ed.ac.uk Tel: +44 131 651 9031

Underwater 3D imaging has a wide range of applications, from seabed mapping to the inspection of subsea substructures [1] and search and rescue missions. While traditionally undertaken using sonar equipment, especially when imaging over long ranges and/or in turbid conditions, an emerging alternative technology is single-photon LIDAR, which promises to surpass the resolution of ultrasound systems while using average optical power of only few 10's of mW.

Single-photon LIDAR illuminates the surveyed area with a pulsed laser source, and detected photons – a combination of ambient photons, laser backscatter from the water (and particles therein), and laser photons reflected from the target – are timed with respect to the laser source. For each scanned point, a photon timing histogram is thereby composed, from which the distance to the target can be estimated. Unlike other optical techniques for 3D imaging, such as active stereo and structured light, single-photon LIDAR enables the backscatter to be separated from the signal from the target, based on the time of arrival of the respective photons.

Existing underwater measurements with single-photon LIDAR have mostly been obtained in experimental water tanks, with recent results including imaging of stationary targets over 7 attenuation lengths [2], imaging of moving targets up to 5.5 AL [3], and real-time 3D reconstruction [4]. The results so far have been predominantly obtained with array format sensors featuring a first-photon TDC architecture, in which pixels only register the timestamp of the first detected photon in every captured frame. This not only imposes limitations on imaging through scattering media (with strong backscatter masking signal photons from the target [5]), but also restricts the effective frame rates that can be achieved due to the inherent bottleneck in having to read out many time stamp frames before a suitable histogram can be formed off-chip.

This paper explores a markedly different SPAD architecture [6] in the context of underwatering imaging, where each pixel has a multi-event TDC and embedded partial histogramming functionality, together with an individual time gate that can be programmed to prescribed positions in time. The sensor, designed originally for free-space LIDAR, comprises of 64×32 pixels, each made up of 4×4 SPADs. Each pixel generates an 8-bin histogram that can be shifted across up to 128 time gate positions, giving a total of 1024 time bins (automated control that locates and tracks the signal peak is also available).

In the present study, an external, 125 MHz clock was used to define the time shift between successive time gate positions, with an adjustable delay line providing the timing for the histogram bins. Calibration was performed for different bin width settings (as obtained by adjusting the voltage applied to the delay line) to account for the per-pixel histogram non-linearity, as well as the left-to-right timing skew in the array resulting from the clock distribution. The calibration process involved the imaging of a flat target, with the trigger signal to the picosecond laser source (532 nm) being swept in time using a digital delay generator (Stanford DG645) over multiple time gate positions. From this measurement, the bin start and end times were estimated for each pixel, and then incorporated into the off-chip histogram processing (centre-of-mass depth extraction [6]). Fig. 1 summarises the calibration process for a given voltage setting. The calibration revealed different time skews for odd and even time gate positions, due to differences in the propagation of rising and falling edges of the external clock (Fig. 2). Fig. 3 shows an example depth map (obtained in free space), again pre- and post-calibration.

With the system calibrated, underwater measurements were taken using an experimental tank (Fig. 4), initially in clear water, and then in increasing scattering conditions via the dilution in water of a commercially available scattering agent (Mucogel). The results, depicted in Figures 5-7 in the form of depth and intensity maps as well as representative histograms, showcase the ability of the system to successfully detect targets at high frame rates even in highly scattering conditions, the depth reconstructions currently being limited by the simple centre-of-mass scheme in use. The signal peak in the histogram was still observed at an AL > 14 (Fig. 8). This represents a significant advance over previous results [2-4], obtained with a first photon TDC, where a maximum AL of 8.3 was demonstrated with similar laser power.

Research is ongoing to develop optimised schemes for extracting the signal peak from histograms which account for the effects of backscatter and forward scatter, enabling more accurate 3D imaging in scattering conditions.

Acknowledgements— This research was supported by Innovate UK (ref. 10004054). AM would like to acknowledge the support of the UK's Royal Academy of Engineering (RF/201920/19/190). The authors are grateful to STMicroelectronics for chip fabrication.

References—

[1] B. Chemisky, et al., Underwater Survey for Oil and Gas Industry: A Review of Close Range Optical Methods. Remote Sens., 2021. 13(14): p. 2789.
[2] A. Maccarone, et al., Three-dimensional imaging of stationary and moving targets in turbid underwater environments using a single-photon detector array. Opt. Express, 2019. 27(20): p. 28437-28456.
[3] A. Maccarone, et al., Submerged single-photon LiDAR imaging sensor used for real-time 3D scene reconstruction in scattering underwater environments. Opt. Express, 2023. 31(10): p. 16690-16708.
[4] S. Plosz, et al., Real-time reconstruction of 3D videos from single-photon LiDaR data in the presence of obscurants. IEEE Trans. Comput. Imaging, 2023, vol. 9, p. 106-119.
[5] S. M. Patanwala et al., "A High-Throughput Photon Processing Technique for Range Extension of SPAD-Based LiDAR Receivers," in IEEE OJ-SSCS, 2022, vol. 2, p. 12-25.
[6] I. Gyongy, et al., A direct time-of-flight image sensor with in-pixel surface detection and dynamic vision. IEEE J. Sel. Top. Quant. Electronics, 2023: p. 1-12.

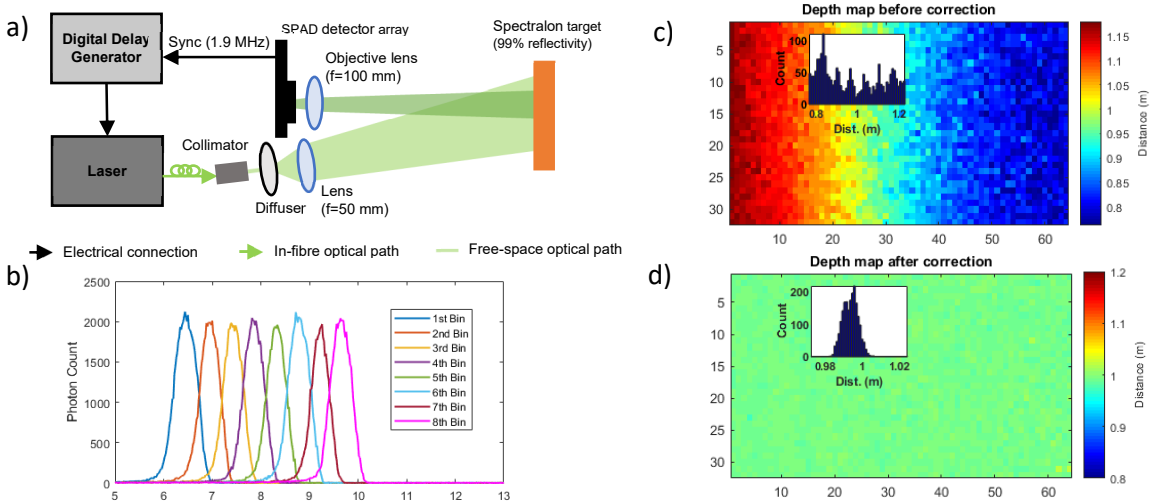

Figure 1. Sensor calibration: a) Block diagram of experimental setup; b) Delay sweep results, obtained with VNDELAY = 790mV, for a representative pixel at a given time gate position, in terms of the responses of the individual histogram bins. The bin start and end times are estimated as the FWHM points of the respective plots; c) depth map before calibration; d) depth map after calibration.

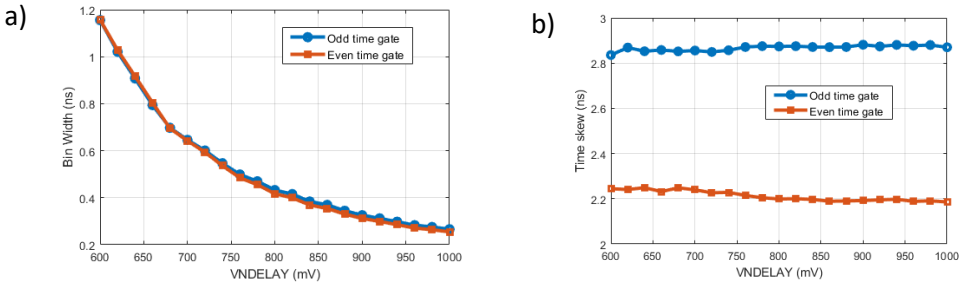

Figure 2. Calibration results: a) average bin width as a function of the VNDELAY voltage applied to the chip; b) right to left time skew as a function of VNDELAY.

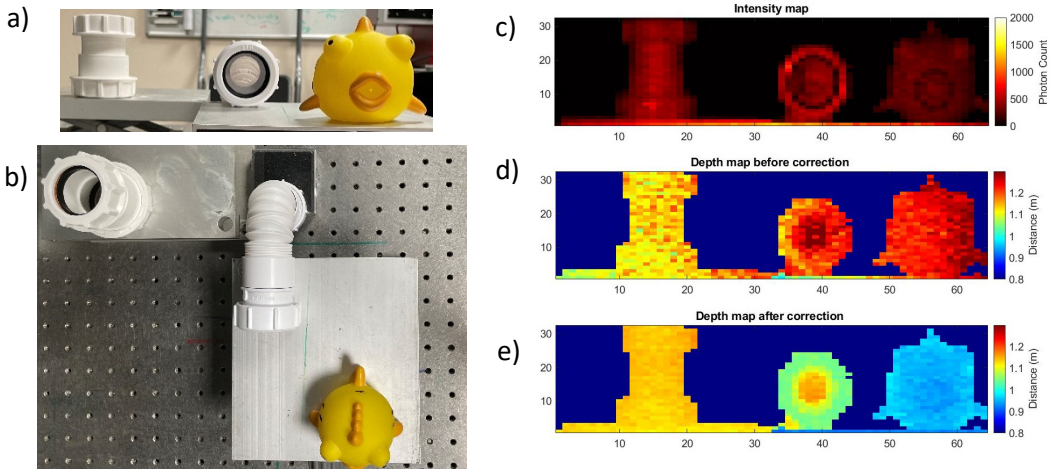

Figure 3. Free-space measurement. Panels a and b show front and top views of the imaged scene. Panel c is an intensity image obtained with the sensor, whereas panels d and e show the depth map before and after calibration. The data was captured with VNDELAY s= 660mV (bin width = 0.83 ns) and an exposure time of 1 ms, resulting in a frame rate of 1 kFPS.

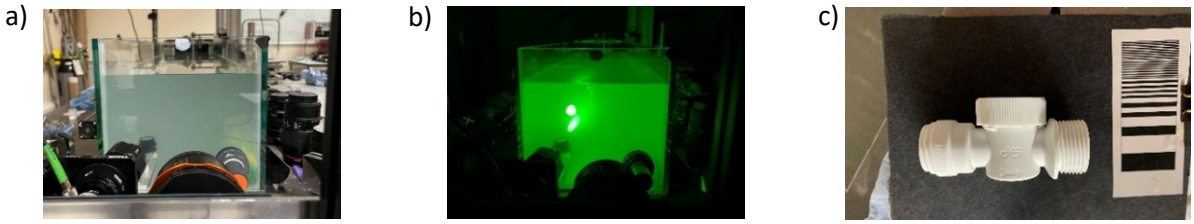

Figure 4. Pictures of the experimental setup for underwater measurements, showing the SPAD camera pointing at the water tank (size 1750 mm × 250 mm × 250 mm), with lights on and off (panels a and b); panel c shows the target at the back of the tank. The picture of the tank was taken in the case of AL = 14.8.

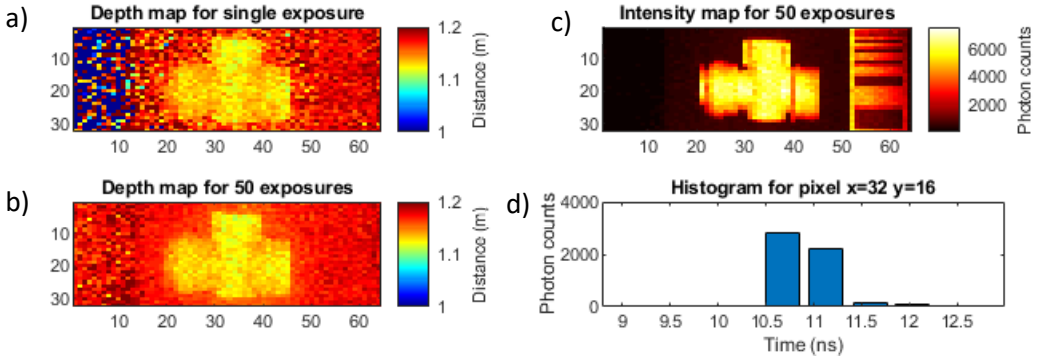

Figure 5. Experimental results in water tank, obtained in clear water: a) depth map for a single 1 ms exposure (1 kFPS); b) depth map for the sum of 50 exposures (equivalent to 20 FPS); c) intensity map (sum of all histogram bins); d) histogram for a central pixel (sum of 50 exposures). The data was captured with VNDELAY = 790mV (bin width = 0.44 ns), and an average optical laser power of P = 2.7 mW.

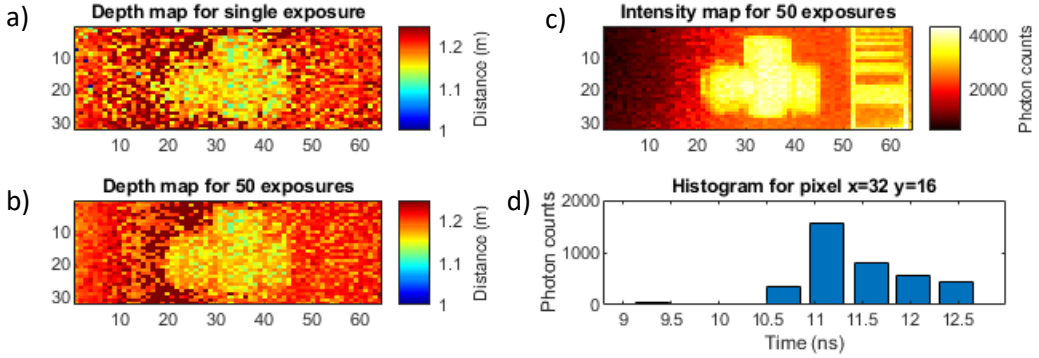

Figure 6. Experimental results in water tank, obtained in AL = 3.03: a) depth map for a single 1 ms exposure (1 kFPS); b) depth map for the sum of 50 exposures (equivalent to 20 FPS); c) intensity map; d) histogram for a central pixel (sum of 50 exposures). An elongated tail is seen in the histogram due to forward scatter. The average optical laser power was P = 19 mW.

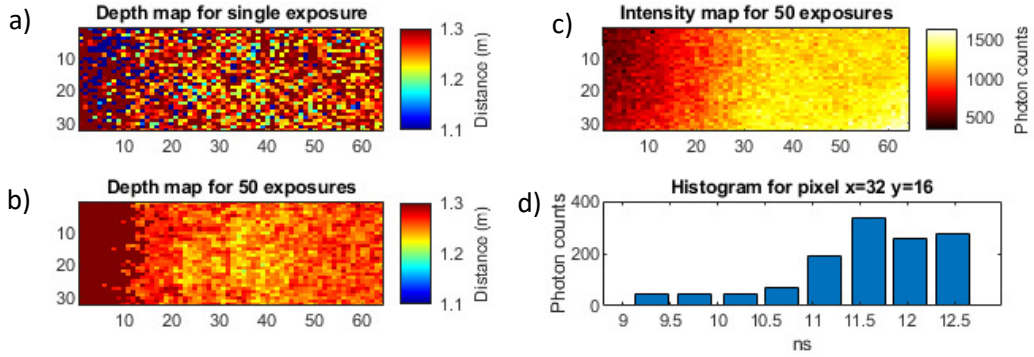

Figure 7. Experimental results in water tank, obtained in AL = 6.07: a) depth map for a single 1 ms exposure (1 kFPS); b) depth map for the sum of 50 exposures (equivalent to 20 FPS); c) intensity map; d) histogram for a central pixel (sum of 50 exposures). Compared to Fig. 6, even stronger forward scatter is evident in the histogram, and elevated counts are seen in the early bins due to backscatter (the backscatter peak is outside the time range of the histogram). The target is still visible (albeit fuzzy) on the depth map but not on the intensity map. P = 32.9 mW.

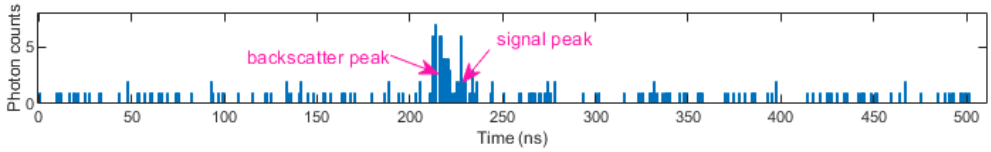

Figure 8. Full histogram for a central pixel obtained by scanning through all 128 time gate positions in AL = 14.2 with a flat Spectralon target. The signal peak can be readily distinguished from the larger, backscatter peak, despite the short exposure time of 1 ms/time gate. P = 29.9 mW.